# Laser cooling, trapping and spectroscopy of calcium isotopes

Mollema, Albert Kornelis

# Chapter 5

# Atom transport: Zeeman slower and deflection stage

## 5.1 Introduction

In this chapter, measurements performed to characterize and optimize the performance of the Zeeman slower and deflection stage are presented. In his thesis, Hoekstra [20] reports on the construction and commissioning of both the Zeeman slower and the deflection stage. These two elements of the experimental set-up are designed to achieve two major goals: atoms evaporated by the oven with velocities up to 1000 m/s should be slowed down to 50 m/s, and out of the original atomic beam, only the desired isotope should be deflected towards the MOT, i.e. the setup should be perfectly isotope selective.

This isotope selectivity of the setup was demonstrated in the recent past [11, 20]. In this chapter, measurements of the velocity distribution of atoms leaving the Zeeman slower are presented. Moreover, as a function of several Zeeman slower and deflection stage parameters the rates of trapping calcium atoms into the MOT have been measured. From this, some conclusions can be drawn about the optimum operation of both parts of the experimental setup.

## 5.2 Characterization of the Zeeman slower

In the case of a thermal expansion where the oven aperture is small compared with the mean free path of the atoms in the oven, the velocity distribution $f(v)$ is given as [40]

$$f(v_z) = \frac{v_z^3}{2\tilde{v}^4} \exp\left(-\frac{v_z^2}{2\tilde{v}^2}\right) \tag{5.1}$$

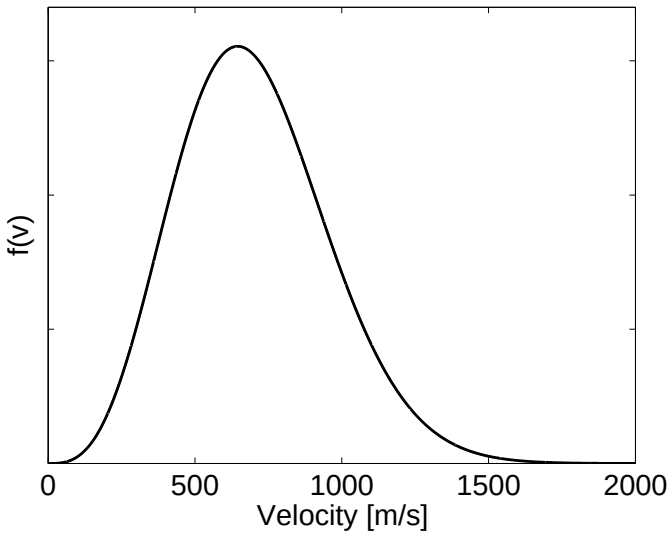


**Figure 5.1:** *Maxwell Boltzmann velocity distribution for $T = 673$ K.*

where $v_z$ is the longitudinal velocity in the atomic beam and the mean velocity $\tilde{v}$ is defined as $\tilde{v} = \sqrt{k_B T/M}$ with $k_B$ Boltzmann's constant, $T$ the temperature and $M$ the mass of the atom. In Fig. 5.1, $f(v)$ is shown for $T = 673$ K. The Zeeman slowing technique is used to slow down part of this initial distribution (up to 1000 m/s) to around 50 m/s.

### Design specifications of the Zeeman slower

As described in the thesis of Hoekstra [20], the design goals of the Zeeman slower were to slow down atoms emitted by the oven with velocities up to 1000 m/s, and decelerate them down to a velocity around 30 to 50 m/s. Simulations were performed to design a magnetic field that would achieve these goals with a laser beam with a power of 30 mW and a detuning of $-370$ MHz [38]. The designed magnetic field and coil structure of the Zeeman slower are shown in Fig. 5.2. This design was eventually implemented. Monte Carlo simulations performed using these parameters predicted that the velocity distribution of atoms leaving the Zeeman slower would be a very narrow (few m/s wide) peak around 50 m/s [38,85]. Predictions for the efficiency of the Zeeman slower (number of atoms slowed to the design final velocity compared to the number of atoms with velocities $\leq 1000$ m/s entering the Zeeman slower) range from 85% [38] to 10% [85]. To verify these simulations we have measured velocity distributions and MOT loading efficiencies for different Zeeman slower settings.

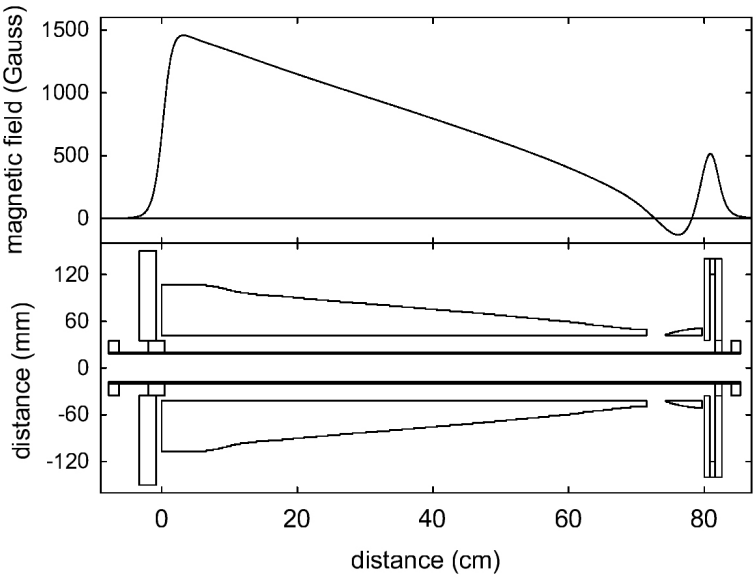


**Figure 5.2:** *Top pannel: Designed Zeeman slower magnetic field, from left to right: the main field ($B > 0$), the dip field ($B < 0$) and the peak field ($B > 0$). Bottom panel: the corresponding coil lay-out. Figure taken from [20].*

### 5.2.1 Velocity distribution of Zeeman slowed atoms

#### Experimental Setup

The velocity distribution after the Zeeman slower was determined by measuring the fluorescence of a tunable probe laser beam intersecting the Zeeman slowed atomic beam at an angle of 60°.

For the experiment, three laser frequencies were needed. Light from the laser was sent through an AOM with a center-frequency of 400 MHz. The $-1$ order was used as the Zeeman slower laser beam. From the 0 order beam, a few mW of laser power was split off to be used directly, without further frequency shifting, for spectroscopy, using the LiPS technique. The spectroscopy signal was used to lock the laser. The rest of the 0 order was sent through a single pass AOM operated at 225 MHz of which the $+2$ order was used. After passing this AOM, the light was sent through a double pass AOM setup, operated at $[150, 250]$ MHz, using the $-1$ order. The laser light was thus shifted by $[-50, 150]$ MHz with respect to the original frequency of the laser light. This beam was used as the probe beam to intersect the Zeeman slowed atomic beam. The fluorescence produced by this probe was measured using a CCD. The diameter of this probe was 1 mm.

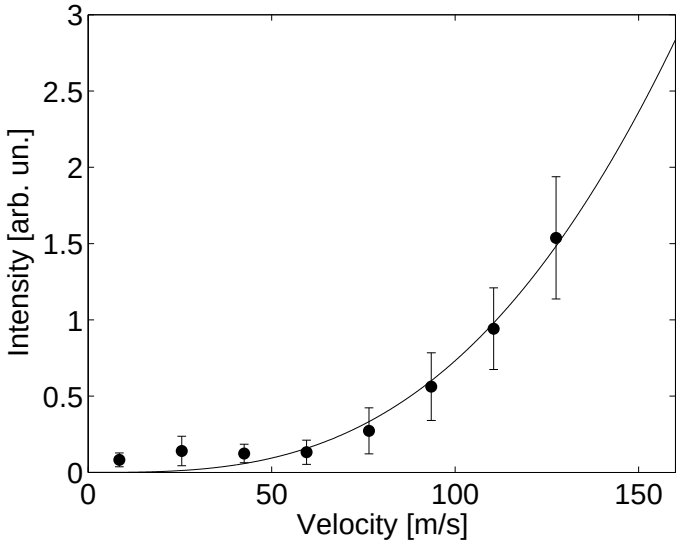


**Figure 5.3:** *Maxwell Boltzmann velocity distribution for $T = 673$ K plotted together with Zeeman slower off data.*

The method used in this experiment is based on the Doppler shift which is given as

$$\nu = \nu_0 \left(1 - \frac{v_L}{c}\right)$$

where $\nu$ is the frequency in the rest frame of the atoms, $\nu_0$ the laser frequency, $v_L$ the velocity component of the atoms parallel to the laser beam and $c$ the speed of light. When the probe beam intersects the atomic beam at an angle $\theta$, we can write

$$v_L = v \cos\theta$$

where $v$ is the longitudinal velocity of the atomic beam. In our experiment the angle $\theta$ is 60°, so it follows that 1 MHz detuning of the probe beam corresponds to 0.85 m/s in longitudinal velocity.

**Experimental procedure**

To measure a velocity distribution spectrum the probe beam was tuned from 10 to 150 MHz in steps of 20 MHz. This frequency range corresponds to velocities of approximately $10-130$ m/s. After changing the frequency of the double pass AOM, care was taken to optimize the alignment and the power of the probe, which was kept at 0.5 mW. Then a CCD picture was taken and the procedure was repeated. For every Zeeman slower setting there was also an image taken while the probe beam was blocked,

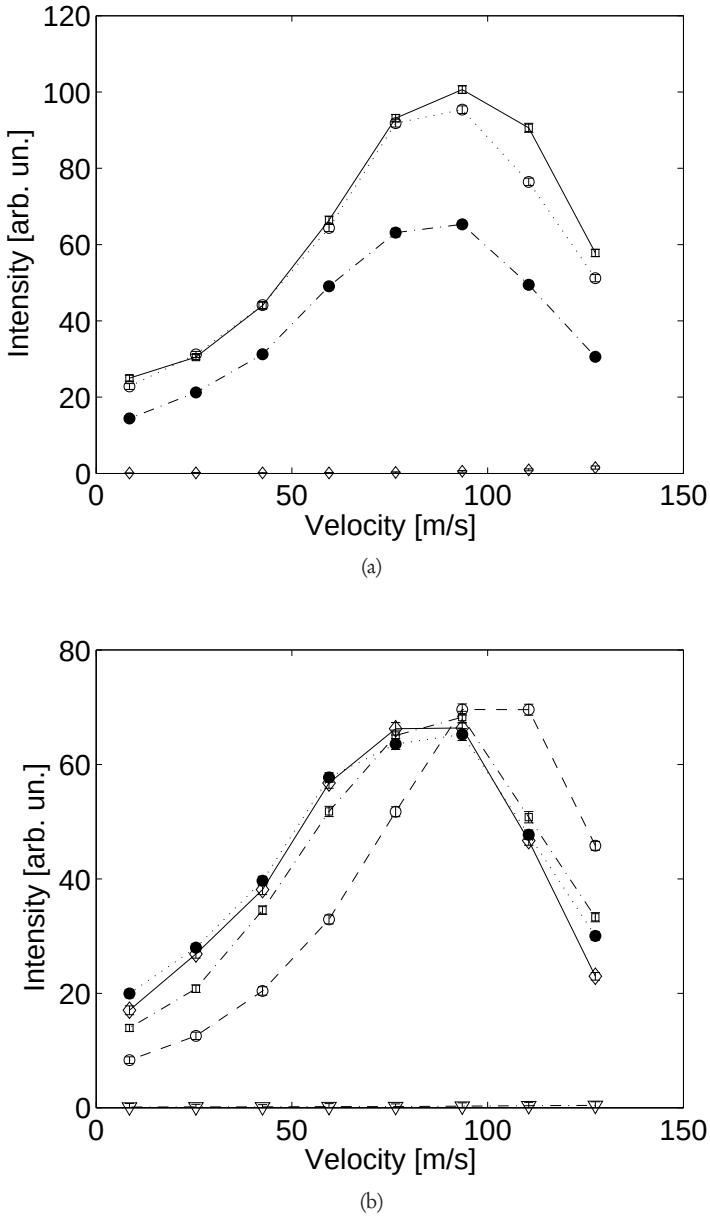


**Figure 5.4:** *(a) Resulting velocity distribution for different peak and dip coil current settings:* $I_{peak} = I_{dip} = 6A$ (□), $I_{peak} = 0$, $I_{dip} = 6A$ (○), $I_{peak} = I_{dip} = 0$ (●), *Zeeman slower laser beam off* (◇). *During these measurements the power of the Zeeman slower laser beam was 40 mW, the detuning* −415 *MHz. (b) Velocity distributions for different Zeeman slower beam powers: 0 mW* (▽) *15 mW* (○), *25 mW* (□), *30 mW* (◇), *35 mW* (●). *During these measurements the detuning was* −415 *MHz and* $I_{peak} = I_{dip} = 0$. *In both (a) and (b) the coil current was 4 A. Lines are connecting points and are drawn to guide the eye.*

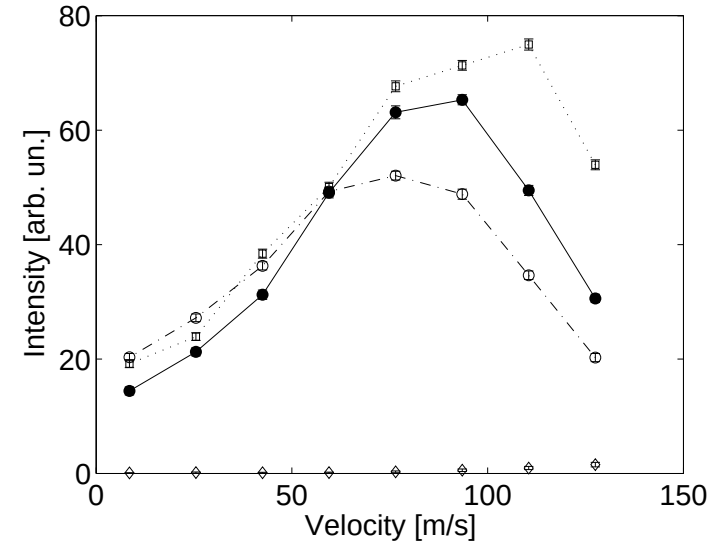


(a)

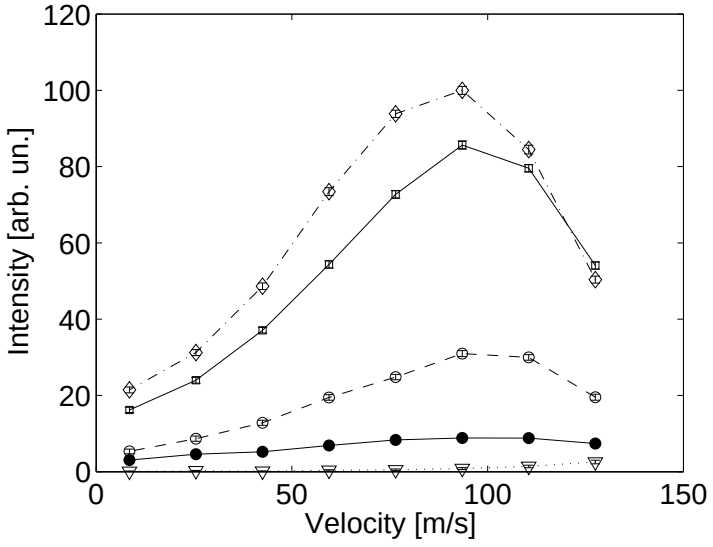


(b)

**Figure 5.5:** *(a) Velocity distributions for different Zeeman slower beam detunings: −435 MHz (□), −415 MHz (●), −395 MHz (○), Zeeman slower laser beam off (◇). During these measurements the power was 40 mW, the coil current was 4 A and $I_{peak} = I_{dip} = 0$. (b) Velocity distributions with different current settings for the main coils of the Zeeman slower: 6 A (◇), 4 A (□), 2 A (○) and 0 A (●), Zeeman slower laser beam off (▽). The power of the Zeeman slower laser beam was 40 mW, the detuning −415 MHz and $I_{peak} = I_{dip} = 0$. In both (a) and (b) lines are connecting points and are drawn to guide the eye.*

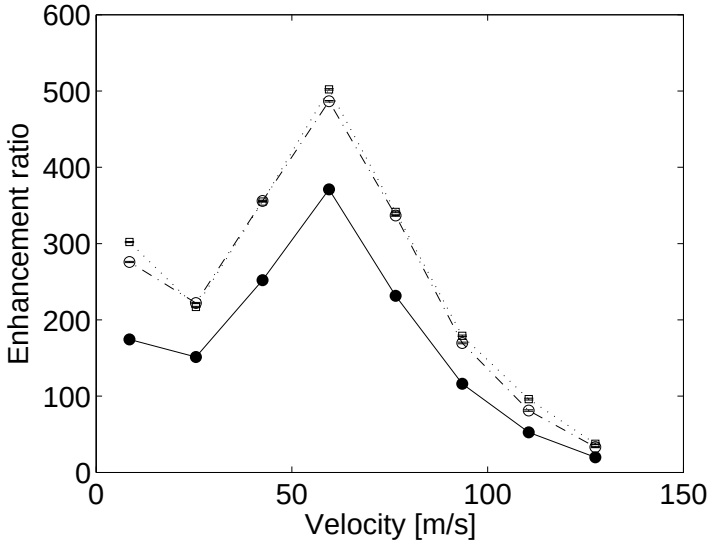


(a)

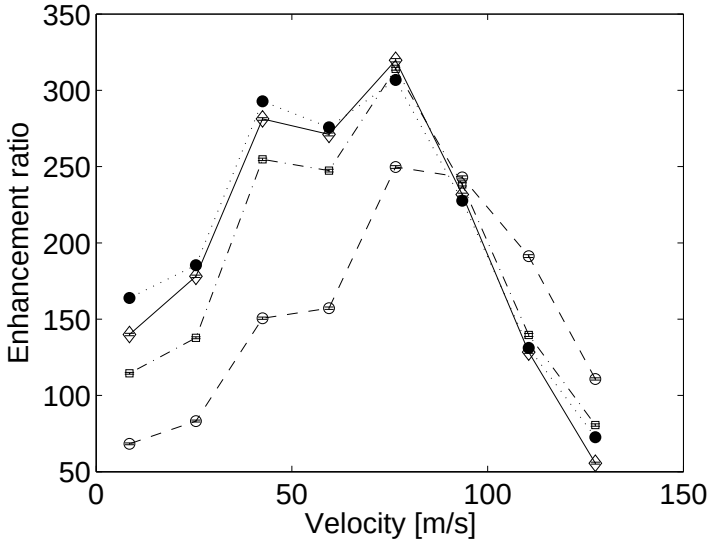


(b)

**Figure 5.6:** *(a) Resulting ratios of Zeeman slower on/off for different peak and dip coil current settings:* $I_{peak} = I_{dip} = 6A$ (□), $I_{peak} = 0$, $I_{dip} = 6A$ (○), $I_{peak} = I_{dip} = 0$ (●). *During these measurements the power of the Zeeman slower laser beam was 40 mW, the detuning −*415 *MHz. (b) Ratios of Zeeman slower on/off for different Zeeman slower beam powers: 15 mW (○), 25 mW (□), 30 mW (◇), 35 mW (●). During these measurements the detuning was −*415 *MHz and* $I_{peak} = I_{dip} = 0$. *In both (a) and (b) the coil current was 4 A. Lines are connecting points and are drawn to guide the eye.*

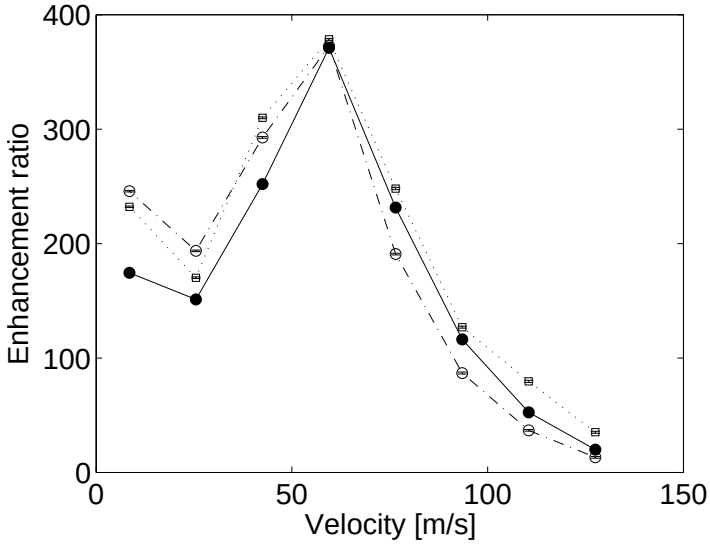


(a)

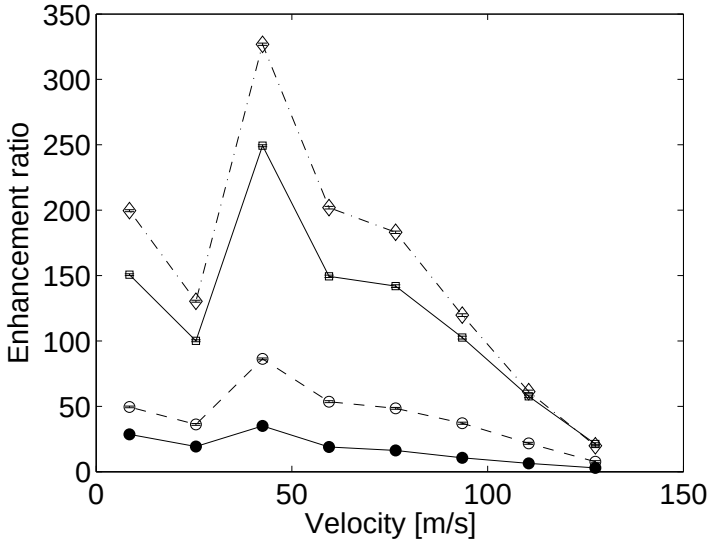


(b)

**Figure 5.7:** *(a) Ratios of Zeeman slower on/off for different Zeeman slower beam detunings:* $-435$ *MHz (□), −415 MHz (●), −395 MHz (○). During these measurements the power was 40 mW, the coil current was 4 A and* $I_{peak} = I_{dip} = 0$*. (b) Ratios of Zeeman slower on/off with different current settings for the main coils of the Zeeman slower: 6 A (◇), 4 A (□), 2 A (○) and 0 A (●). The power of the Zeeman slower laser beam was 40 mW, the detuning* $-415$ *MHz and* $I_{peak} = I_{dip} = 0$*. In both (a) and (b) lines are connecting points and are drawn to guide the eye.*

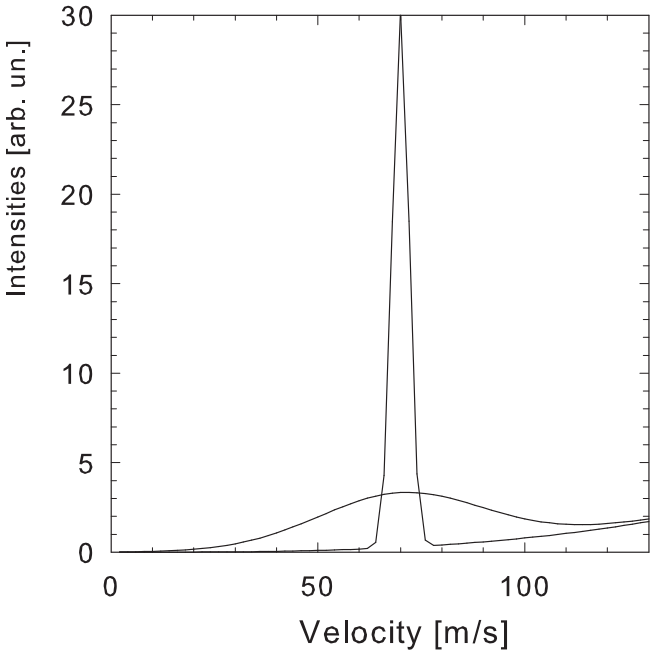


**Figure 5.8:** *Illustration of peak broadening as due to the linewidth of the transition and power broadening. The narrow peak represents the actual velocity distribution of the atoms, the broadened one the observed peak (see text for more details).*

in order to have the opportunity to do proper background subtraction during the off line analysis of the data.

The influences of three Zeeman slower parameters were studied: the value of the peak coil current, the power of the Zeeman slower laser beam and the detuning of the Zeeman slower laser beam.

### Data analysis

The exact location of the intersection between the atomic beam and the probe was determined by combining the information from pictures with and without a probe. A box of 4 by 4 pixels was taken around this location, from which the average pixel value was calculated. This way we can be sure that only the longitudinal velocity distribution is probed.

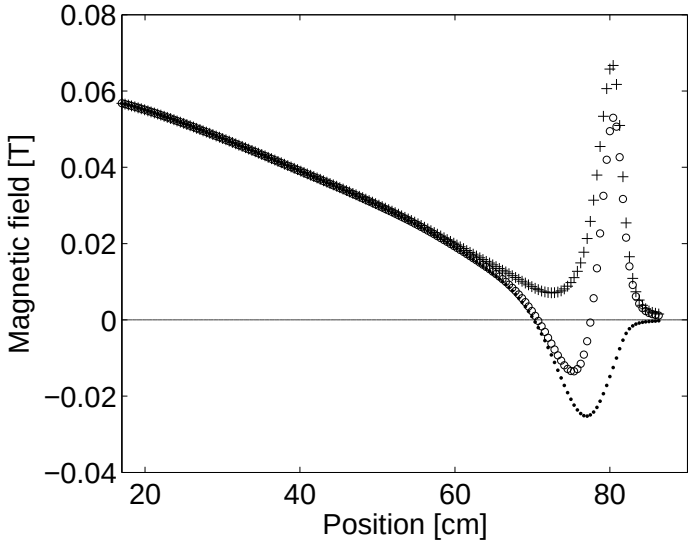


(a)

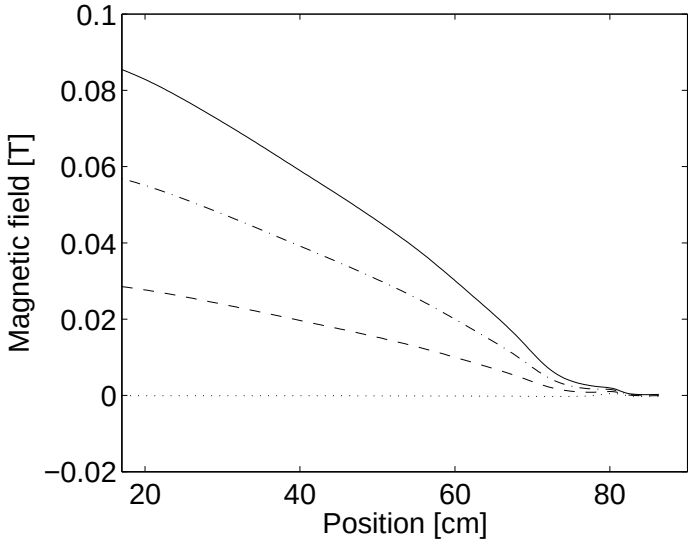


(b)

**Figure 5.9:** *(a) (Measured Zeeman slower magnetic fields for different peak and dip coil current settings:* $I_{peak} = I_{dip} = 6A$ (○), $I_{peak} = 0$, $I_{dip} = 6A$ (●), $I_{peak} = 6, I_{dip} = 0$ (+). *In all cases the main coil current was 4 A. (b) Measured Zeeman slower fields for different main coil current settings: 6 A (full), 4 A (dashdotted), 2 A (dashed), 0 (dotted).*

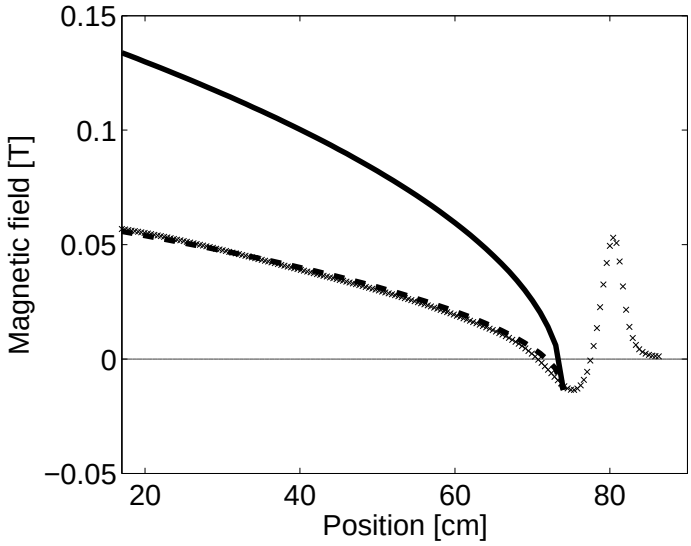


**Figure 5.10:** *Zeeman slower magnetic field measured with coil current 4 A and peak and dip currents of 6 A (×). Also drawn are the square root shaped magnetic field calculated using Eq. 2.27 with initial velocities 1000 m/s (full line) and 470 m/s (dashed line) and $z_0 = 75$ cm, which is the length of the Zeeman slower.*

### Results and discussion

First of all the velocity distribution at the end of the Zeeman slower was measured while the Zeeman slower was off. The data of this measurement, presented in Fig. 5.3 show good agreement with the expected velocity distribution of a beam from an oven at 673 K.

The results of the velocity distribution measurements for different settings of the magnetic field and laser intensity and detuning are given in Fig. 5.4 and 5.5. Clear enhancement of atoms with $v < 150$ m/s was found. The peaks of the velocity distributions are found between 60 and 100 m/s (which is roughly 50% above the design value). From Fig. 5.4(a) it seems that changing the peak and dip currents does not change the width and peak position of the velocity distribution too much, but rather its amplitude. From Fig. 5.4(a) it can be concluded that the velocity distributions for laser powers of $25 - 35$ mW are nearly the same. However, as will be shown later, the MOT yields are still increasing at laser powers between 25 and 30 mW. The data shown in Fig 5.5(b) suggest that more atoms are slowed down when the coil current is increased to 6 A. Unfortunately the current through the coils during normal operation was limited to 4 A since proper cooling with the existing water cooling system could not be guaranteed for higher currents.

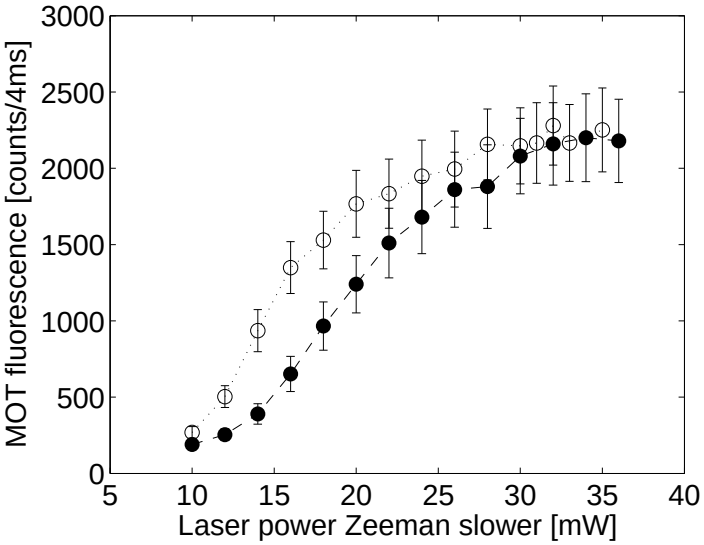


**Figure 5.11:** *MOT yield as function of Zeeman slower laser beam power when the dip current was optimized for 30 mW (●) and when the dip current was optimized for every power setting (○). Lines are connecting points and are drawn to guide the eye.*

In Figs 5.6 and 5.7 the ratios for Zeeman slower on/off are given. The flux enhancement without peak and dip current is approximately 300 for optimal intensity and detuning parameters. When the peak and dip current is on, the enhancement factor increases to approximately 500. Interestingly, to obtain this enhancement it seems to be sufficient to switch on either one of the peak or dip coils. It is of note that the highest enhancements are obtained near the design velocity of 50 m/s.

The width of the velocity distribution found in the simulations is in the order of $5-10$ m/s. The observed width in the velocity distributions is in the order of 60 m/s. The observed widths can for the better part be understood from the linewidth of the used transition (34.6 MHz) and its enhancement due to power broadening which yields a total linewidth of $\Gamma_p = \Gamma\sqrt{1+s_0} \approx 45$ MHz. This corresponds to a width in the velocity distribution of $\sim 40$ m/s, see Fig. 5.8 for an illustration. Due to this broadening, the enhancement ratios obtained from the velocity distributions are likely to be underestimated strongly. Assuming that the final distribution is a narrow one of about $5-10$ m/s FWHM, the enhancement at the peak velocity is certainly a factor of 10.

The actual magnetic field strengths and shapes present in the Zeeman slower during the measurements described above are shown in Fig. 5.9. The field as a function of position in the Zeeman slower was measured using a Hall probe. Due to practical limitations of the field meter setup the first $\sim$ 15 cm of the Zeeman slower magnetic

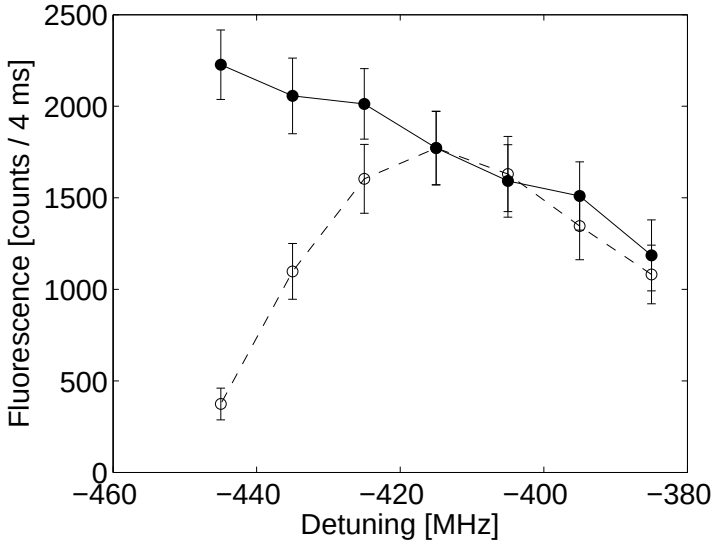


**Figure 5.12:** *MOT yield as function of Zeeman slower laser detuning when the peak and dip currents were optimized for* −415 *MHz (○) and when the peak and dip currents were optimized for every detuning (●). Lines are connecting points and are drawn to guide the eye.*

field could not be measured and is not shown in the figures.

The velocity $v$ that atoms should have to be in resonance with the laser at the end of the Zeeman slower can, if the magnetic field $B$ and the detuning of the laser with respect to the transition frequency in the rest frame of the atom $\delta$ are known, be calculated from the equation

$$v = \frac{\mu' B/\hbar - 2\pi\delta}{k} \tag{5.2}$$

If the main, peak and dip currents are 4, 6 and 6 A respectively the field at the end of the Zeeman slower is −135 G. If $\delta = -415$ MHz it can be calculated that $v = 94$ m/s. This is in excellent agreement with the measured peak velocity of $\sim$ 95 m/s for the corresponding Zeeman slower settings (cf. Fig. 5.4(a), squares). If, however, the dip current is zero and therefore the field at the end of the Zeeman slower $B \approx 0$ a final velocity of 170 m/s is expected. The position of the measured peak for this setting (Fig. 5.4(a)) is hardly shifted.

A similar test can be performed for different detunings of the Zeeman slower laser beam, of which the velocity distribution data is presented in Fig. 5.5(a). According to Eq. 5.2 the final velocity should decrease by 8.5 m/s if the detuning is changed by 20 MHz. This trend seems to be in agreement with the data.

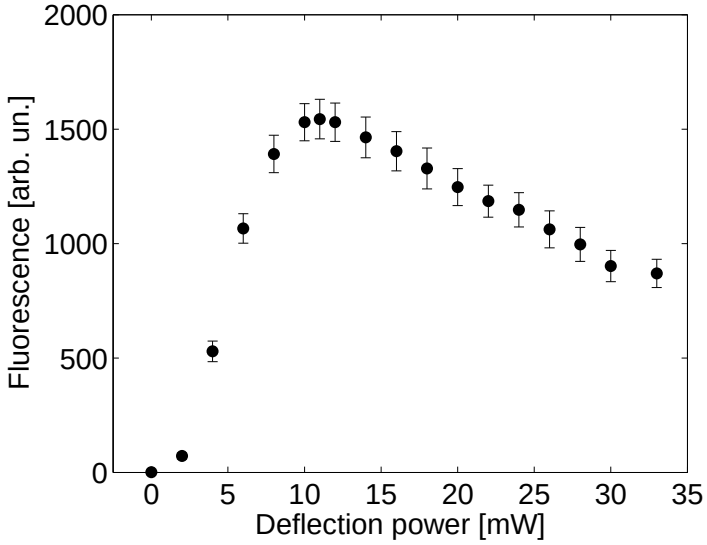


**Figure 5.13:** *MOT yield as function of deflection laser power.*

The magnetic field typically used for normal operation of the Zeeman slower is shown in Fig. 5.10, together with magnetic fields calculated using Eq. 2.27:

$$B(z) = B_b + B_0\sqrt{1 - z/z_0}.$$

Assuming that this equation is correct, the comparison between the measured and calculated fields clearly shows that the typical magnetic field used does not slow down atoms with velocities up to 1000 m/s but is in excellent agreement with a calculated field for atoms with initial velocities up to 470 m/s instead.

## 5.2.2 MOT yield as a function of Zeeman slower settings

### Zeeman slower laser power

In order to determine the optimum Zeeman slower laser power the MOT yield was measured as a function of laser power. In this experiment, atoms were slowed down in the Zeeman slower, operating at a total detuning of −400 MHz and deflected into the MOT. The laser power of the deflection stage was 10 mW. The detuning of both the MOT and deflection laser light was −36 MHz (∼ 1Γ) and the MOT was operated at $s_0 = 0.14$. Two experiments were performed: in one experiment the current of the dip coil was optimized for a laser power of 30 mW and kept at that setting while the MOT yield was measured for several laser powers. In a second experiment, the dip current was optimized for every laser power setting. Both data sets are shown in Fig. 5.11.

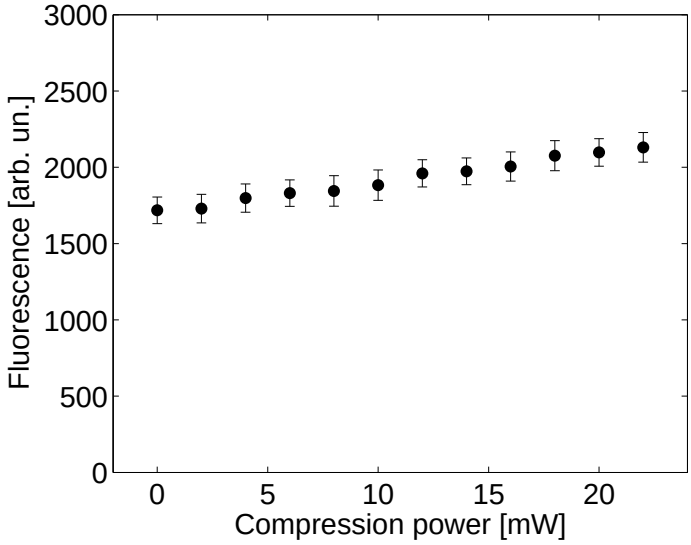


**Figure 5.14:** *MOT yield as function of compression laser power.*

### Zeeman slower laser detuning

A similar experiment as described above was performed to measure the MOT yield as function of the Zeeman slower laser detuning. The laser power of the deflection stage was 11 mW. The detuning of both the MOT and deflection laser light was $-36$ MHz ($\sim 1\Gamma$) and the MOT was operated at $s_0 = 0.17$. Two experiments were performed: in one experiment the currents of the dip and peak coil were optimized for a laser detuning of $-415$ MHz and kept at that setting while the MOT yield was measured for several Zeeman slower laser detunings. In a second experiment, the dip and peak currents were optimized for every Zeeman slower laser detuning. Both data sets are shown in Fig. 5.12.

### Results and discussion

From Figs 5.11 and 5.12 it can be concluded that a possible change for the worse caused by changing the Zeeman slower parameters detuning and power can for a large part be corrected for by changing the peak/dip settings. From Fig. 5.4(a) it seems that changing the peak and dip currents does not change the width and peak position of the velocity distribution too much, but rather its amplitude.

## 5.3 Deflection stage and compression measurements

### MOT yield as function of deflection power

To determine the optimum laser power needed for the deflection of the atoms towards the MOT, the MOT fluorescence was measured as a function of deflection laser power. Atoms were slowed down with the Zeeman slower (laser power 25 mW, detuning −415 MHz, coil current 4 A, peak and dip coil currents optimized) and deflected by the deflection stage using laser powers in the range from 0 to 34 mW. The detuning of the MOT and the deflection was −36 MHz and the $s_0$ of the MOT was 0.16. The result is given in Fig. 5.13.

### MOT yield as function of compression power

A substantial part of the atoms evaporated by the oven are assumed to be lost in the part of the setup between the oven and the deflection, mainly due to the divergence in the atomic beam. Compressing the beam before it enters the Zeeman slower by means of an optical molasses might be a cure to this issue. To explore the possibilities to reduce the loss of atoms this way the following experiment was set up. A retro-reflected laser beam with a radius of $\sim$ 1 cm crossed the atomic beam right after the oven (so just before it enters the Zeeman slower). The MOT yield is now measured as a function of the power of this laser beam. Results of the experiment are given in Fig. 5.14.

### Discussion

In Fig. 5.13 the MOT yield shows a clear maximum at a laser power of 11 mW. The decrease in MOT yield at higher deflection laser powers may be due to diffusive heating of the atomic beam in the plane perpendicular to the plane in which the deflection takes place which is a result of the increasing photon scattering rate. The same heating effect also plays a role when atoms are trapped in a MOT, where it is reflected in a higher temperature of the trapped atoms (cf. Chapter 6). Adding an extra retro-reflected laserbeam perpendicular to the current deflection beam might solve this problem. Unfortunately, the influence of the deflection parameters on the velocity distribution of the deflected atoms could not be determined.

The gain in MOT yield resulting from the compression before the Zeeman slower is rather small, given the amount of laser power needed. Alternative schemes for compression could not be applied for several reasons. A multi-pass scheme, as described by Hoogerland et al. [86] was tried but the approach failed due to problems with reflections from the vacuum windows. A curved wavefront technique, see e.g. Rooijakkers et al. [87], could not be applied because of the high saturation intensity of the cooling transition in Ca.

## 5.4 Conclusion

In this Chapter we have shown that with the current Zeeman slower enhancement ratios up to 500 m/s can be reached. However, the actual velocity distributions of atoms leaving the Zeeman slower are not in agreement with the design goals of the Zeeman slower [20] nor with the simulations presented in Refs. [38, 85]. The position of the peak maximum appears to be somewhere between $60 - 100$ m/s for all Zeeman slower parameters studied, while the design goal was to slow down the atoms to around 50 m/s. Simulations using the implemented design parameters predicted velocities around 50 m/s as well. We can therefore conclude that not all the processes taking place in the Zeeman slower are well described in the simulations.

Based on the magnetic field at the end of the Zeeman slower and the detuning of the Zeeman slower laser beam, the velocity of the atoms needed to be in resonance with the laser at that point can be calculated. In principle, this is the final velocity of the atoms at the end of the Zeeman slower. This nicely explains the trend in the apparent peak position as a function of laser detuning in Fig. 5.5(a). On the other hand the effect expected as a function of Zeeman slower exit field is not present in the data of Fig. 5.4(a). The precise influence of the end field on the velocity distribution therefore remains to be understood.

The magnetic field of the Zeeman slower that is used for normal operation (coil, peak and dip currents being 4, 6 and 6 A respectively) was measured. Comparison of the measured field with the theoretical optimum field shape that can be calculated using Eq. 5.10 reveals that the maximum initial velocity of the atoms that can be slowed down by the Zeeman slower is in the order of 470 m/s. To reach its design criterium of decelerating atoms from 1000 m/s it will be necessary to be able to operate the main coil of the Zeeman slower at 8 A without overheating the coil.

The deflection power vs. MOT yield measurements in Fig. 5.13 show a clear optimum at 11 mW. It is assumed that the decrease of MOT yield at higher deflection laser powers is due to diffusive heating of the atomic beam. Further increase of the MOT yield might be expected from adding compressing laser beams perpendicular to the deflection beams. Current measurements could, unfortunately, not reveal which part of the velocity distribution of the atoms leaving the Zeeman slower is actually deflected nor could it be determined how the velocity distribution of the atoms is affected by the deflection stage. The gain in MOT yield resulting from compression of the atomic beam before the Zeeman slower is rather low. This might be due to the fact that the average interaction time of the laser beams with the atoms is rather short due to the high velocity of the atoms right after the oven and/or to lateral heating during slowing of the beam in the Zeeman slower. Other compression schemes before the Zeeman slower could not be tried due to technical limitations. A compression stage after the Zeeman slower could be an efficient tool to reduce the transverse heating in the Zeeman slower. Reducing the divergence of the slowed-down atom beam will definitely improve the transport from Zeeman slower to the MOT.